Effects of Modification of Calcium Hydroxyapatites by Trivalent Metal Ions on the Protein Adsorption Behavior

Kazuhiko Kandori,*,† Satoko Toshima,† Masato Wakamura,‡ Masao Fukusumi,§ and Yoshiaki Morisada§

School of Chemistry, Osaka University of Education, 4-698-1 Asahigaoka, Kashiwara-shi, Osaka, 582-8582, Japan, Environmental Technology Laboratory, Device & Material Laboratories, Fujitsu Laboratories Ltd., 10-1 Morinosato-Wakamiya, Atsugi 243-0197, Japan, and Department of Processing Technology, Osaka Municipal Technical Research Institute, 1-6-50 Morinomiya, Joto-ku, Osaka 536-8553, Japan

Received: December 13, 2009; Revised Manuscript Received: January 11, 2010

The effects of modification of calcium hydroxyapatites (Hap; $Ca_{10}(PO_4)_6(OH)_2$) by trivalent metal ions (Al(III), La(III), and Fe(III)) on protein adsorption behavior were examined using bovine serum albumin (BSA; isoelectric point (iep) = 4.7 and molecular mass (M_s) = 67 200 Da). The Al(III)-, La(III)-, and Fe(III)-substituted Hap particles were prepared by the coprecipitation method with different atomic ratios, metal/(Ca + metal), abbreviated as X_{metal}. The particles precipitated at $X_{metal} = 0$ (original-Hap) were rod-like and 10 × 36 nm^2 in size. The short, rod-like original-Hap particles were elongated upon adding metal ions up to $X_{metal} = 0.10$, and the extent of the particle growth was in the order of La(III) < Al(III) ≪ Fe(III). The crystallinity of the materials was slightly lowered by increasing X_{metal} for all systems. The adsorption isotherms of BSA onto the Al(III)-, La(III)-, and Fe(III)-substituted Hap particles showed the Langmuirian type. The saturated amounts of adsorbed BSA (n_s^{BSA}) values were strongly dependent on X_{metal} in each system. The n_s^{BSA} values for the Fe(III)-substituted Hap system were increased with an increase in X_{Fe} (X_{metal} value of Hap particles substituted with Fe(III)); the n_s^{BSA} value obtained at $X_{Fe} = 0.10$ was 2.7-fold more than that for the original-Hap particle, though those for the La(III) system were decreased to ca. 1/5. On the other hand, the n_s^{BSA} values for the Al(III) system were decreased with substitution of small amounts of Al(III), showing a minimum point at $X_{Al} = 0.01$, but they were increased again at X_{Al} over 0.03. Since the concentrations of hetero metal ions dissolved from the particles exhibited extremely low values, the possibility of binder effects of trivalent cations dissolved from the particle surface for adsorbing BSA to trivalent-ion-substituted Hap particles was excluded. The increase of n_s^{BSA} by an increase in X_{Fe} was explained by elongation of mean particle length along with the production of surface hydroxo ions, such as $Fe(OH)^{2+}$ or $Fe(OH)_2^{+}$, to induce the hydrogen bond between the Fe(III)-substituted Hap surface and BSA molecules, though the number of original **C** sites established by Ca(II) atoms was reduced. In the case of La(III)-substituted Hap particles, the number of original **C** sites established by Ca(II) atoms was reduced by La(III) substitution but the mean particle length remained almost constant. Furthermore, surface hydroxo La(III) groups were absent. Therefore, the reduction of n_s^{BSA} was explained by both the unaltered mean particle length and their low surface hydrophilicity. The change of n_s^{BSA} values by X_{Al} resembled that of the mean particle length. These results implied that both the mean particle length and surface hydrophilicity of Al(III)-, La(III)-, and Fe(III)-substituted Hap particles are determining factors of the adsorption amounts of BSA.

Introduction

It is well-known that a synthetic calcium hydroxyapatite $Ca_{10}(PO_4)_6(OH)_2$, designated as Hap, attracts attention as bioceramics, acid−base catalysis in various reactions, and adsorbents for separation of biomaterials. Hap is in the space group $P6_3/m$; its unit cell parameters are $a = b = 0.943$ nm and $c = 0.688$ nm, and it possesses two different binding sites (**C** and **P** sites) on the particle surface, as is depicted the crystal structure of Hap in Figure 1. Thus, it contains a multiple-site binding character for proteins.[1−3] After dispersing Hap particles in aqueous media, calcium atoms (Ca(II) atoms in Figure 1a) are exposed on the Hap surface by dissolution of OH^- ions at the particle surface to produce rich in calcium ions or positively charged sites to bind to acidic groups of proteins, so-called **C** sites. These **C** sites are arranged on the *ac* or *bc* particle face in a rectangular manner with interdistances of 0.943 and 0.344 nm (*c*/2) for the *a* (or *b*) and *c* directions, respectively (Figure 1a). Chen et al. reported that the $-COO^-$ claw of the protein grasps the calcium atoms of the Hap surface with its two oxygen atoms in a triangle form.[4] Shaw et al. also revealed that the $-COO^-$ terminus of amelogenin is orientated to the Hap surface by using solid state NMR study.[5] The **P** sites, negatively charged adsorbing sites, each formed by six oxygen atoms belonging to three crystal phosphate ions, are arranged hexagonally on the *ab* particle face with a minimal interdistance in both *a* and *b* directions equal to $|a| (=|b|) = 0.943$ nm (Figure 1b). In addition, Hap is the most stable calcium phosphate under physiological

* Author to whom all correspondence should be addressed. E-mail: kandori@cc.osaka-kyoiku.ac.jp.
† Osaka University of Education.
‡ Fujitsu Laboratories Ltd.
§ Osaka Municipal Technical Research Institute.

10.1021/jp911783r
Published on Web 02/03/2010

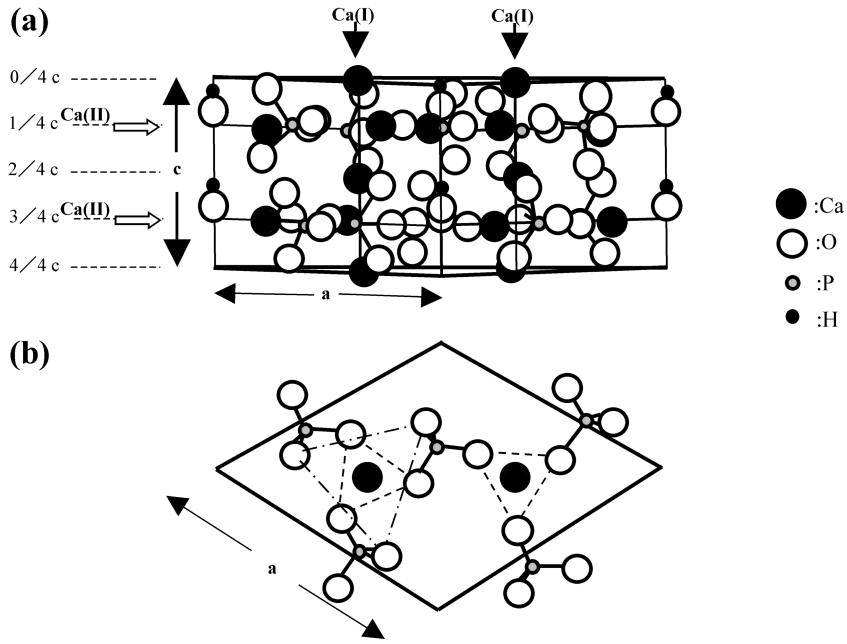

Figure 1. (a) Projection of the unit cell of Hap crystal viewed along the [110] face and (b) surface structure of the *c* crystal surface viewed along the [001] face.

conditions. Hence, Hap is widely applied for separating various proteins using as a column for a high-performance liquid chromatograph (HPLC) apparatus and many essential studies have been reported.[2,6,7]

In the past decade, the authors' group has conducted fundamental studies on the adsorption of acidic bovine serum albumin (BSA), neutral myoglobin (MGB), and basic lysozyme (LSZ) onto various kinds of synthetic Hap particles.[8–16] In these studies, we investigated by changing many factors of Hap particles, such as calcium-to-phosphorus (Ca/P) atomic ratio, kinds of divalent cations (Ca, Sr, and Ca−Sr solid solution), mean particle length, contents of carbonate ions incorporated and heat treatment temperature. To our best knowledge, however, no study has been reported on the effect of modification of Hap particles by trivalent metal ions on the protein adsorption behaviors. One of the authors already reported that the surface structure and composition of Hap particles produced by the coprecipitation method are drastically changed by substitution with trivalent Al(III), La(III), and Fe(III) ions.[17] The previous paper revealed that Fe(III) atoms replace Ca(II) ones as hydroxo ions and the substitution with La(III) ions accompanies OH^- deficiency. In situ FTIR spectra measurement indicated that the Hap particles substituted with Al(III) and Fe(III) possess surface Al−OH and Fe−OH groups besides the surface P−OH ones, whereas the Hap substituted with La(III) has no surface La−OH group. From these results, it can be expected that the adsorption behaviors of proteins drastically change by modification of Hap with trivalent metal ions because adsorption behavior is only governed by the surface structure of adsorbents. To explore this subject and to extend the previous work, we investigated the adsorption behavior of BSA onto Al(III)-, La(III)-, and Fe(III)-substituted Hap particles disclosed before.[17] The results obtained in the present study must serve not only to elucidate the interaction of proteins to trivalent-metal-ion-substituted Hap particles but also to produce a high-quality HPLC column and may be useful to the researchers in the fields of biomaterials, biomineralization, and biosensors.

Experimental Section

Materials and Methods. Previously prepared colloidal Hap particles substituted with varied amounts of trivalent metal ions were used in this study. These particles were prepared by the coprecipitaton reactions of $Ca(NO_3)_2$ and H_3PO_4 in aqueous solutions containing varied amounts of Al(III), La(III), and Fe(III) nitrates as the authors already reported elsewhere.[17] The substitution with metal ions was done at different atomic ratios ranging from 0 to 0.10 in metal/(Ca + metal), called X_{metal} hereafter. Also, X_{Al}, X_{La}, and X_{Fe} mean the X_{metal} values substituted with Al(III), La(III), and Fe(III), respectively. The Hap particles generated were filtered off, thoroughly washed with distilled water, and finally dried at 70 °C in an air oven for 24 h.

Characterization. The shape, specific surface area, crystal phase, and Ca^{2+} and PO_4^{3-} contents of Hap particles were determined by a transmission electron microscope (TEM), N_2 and H_2O adsorption measurements, X-ray diffraction (XRD), X-ray photoelectron spectroscopy (XPS), and inductively coupled plasma atomic emission spectroscopy (ICP-AES). The adsorption isotherm of N_2 was measured at the boiling point of liquid nitrogen with the use of a computerized automatic volumetric apparatus built in-house. Adsorption isotherms of H_2O were also determined by a gravimetric technique at 25 °C. Specific surface areas were obtained by fitting the BET equation to these N_2 and H_2O adsorption isotherms and were abbreviated as S_N and S_W, respectively. Prior to these gas adsorption measurements, the samples were evacuated at 300 °C for 2 h. The XRD patterns were taken with Ni-filtered Cu K_α radiation (40 kV, 120 mA). The conditions for production of Al(III)-, La(III)-, and Fe(III)-substituted Hap particles are listed in Table 1.

Protein Adsorption Measurement of BSA. The amounts of BSA adsorbed on Al(III)-, La(III)-, and Fe(III)-substituted Hap particles were measured by a batch method as following the method employed in our previous papers.[12–14,16] This measurement was conducted at 15 °C employing a 1×10^{-4} mol/dm^3 KCl solution of the protein in 10 cm^3 Nalgen polypropylene centrifugation tubes. The centrifugation tubes

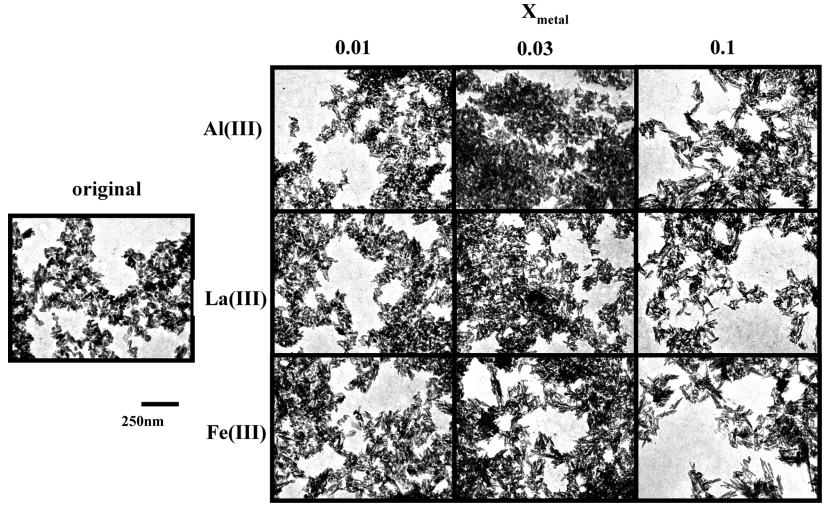

Figure 2. TEM pictures of the particles formed at varied X_{metal} by the coprecipitation method.

TABLE 1: Properties of Al(III)-, La(III)-, and Fe(III)-Substituted Hap Particles

sample	X_{metal}	X_W (in particle)	X_S (in surface)	X_S/X_W	S_N (m^2/g)	S_W (m^2/g)	S_W/S_N	size (nm)
original	0				92	70	0.76	36 × 10
Al(III)	0.01	0.014	0.060	4.3	124	122	0.99	25 × 7
	0.03	0.042	0.050	1.2	127	102	0.80	51 × 6
	0.1	0.126	0.077	0.6	147	109	0.74	76 × 5
La(III)	0.01	0.013	0.028	2.2	125	89	0.71	42 × 5
	0.03	0.041	0.054	1.3	166	114	0.69	39 × 4
	0.1	0.160	0.114	0.7	173	115	0.67	47 × 3
Fe(III)	0.01	0.016	0.016	1.0	102	118	1.15	55 × 5
	0.03	0.054	0.037	0.7	141	149	1.05	69 × 5
	0.1	0.130	0.056	0.4	122	165	1.35	150 × 5

were gently rotated end-overend at 15 °C for 48 h in a thermostat. The concentrations of proteins were measured by the microbiuret method using an UV absorption band at 310 nm after centrifuging the dispersions. Most of the UV experiments were triplicated and reproducible within 2%, indicating an uncertainty of 2×10^{-2} mg/m^2 for the amounts of BSA adsorbed. The zeta potential (zp) of the BSA adsorbed particles was also measured by an electrophoresis apparatus. BSA was purchased from Sigma Co. (A-7030). The isoelectric point, molecular weight and size of BSA are 4.7, 67 200 Da, and 4.0 × 14.0 nm^2, respectively.

Results and Discussion

Properties of Hap Particles. The TEM pictures of Al(III)-, La(III)-, and Fe(III)-substituted Hap particles used in this study are shown in Figure 2. The particles precipitated at $X_{metal} = 0$ (original-Hap) are rod-like and 10 × 36 nm in size. The Ca/P atomic ratio of the original-Hap was 1.59, suggesting that the particles are calcium deficient. As seen in Figure 2, the short rod-like original-Hap particles are elongated upon adding metal ions up to $X_{metal} = 0.10$ and the extent of the particle growth is in the order of La(III) < Al(III) ≪ Fe(III). In Figure 3 is plotted the mean particle length estimated from TEM images against X_{metal}. It is seen that the effect of Fe(III) on the growth of Hap particle is more remarkable than those of Al(III) and La(III). It should be noticed here that the mean particle length in the Al(III) system shows a minimum at $X_{Al} = 0.01$, suggesting that particle growth in the presence of small amounts of Al(III) ions was inhibited. However, the reason for this fact remains unclear at the present. The properties of Al(III)-, La(III)-, and Fe(III)-substituted Hap particles employed in this paper are summarized in Table 1. The X_s and X_w values in this table represent the

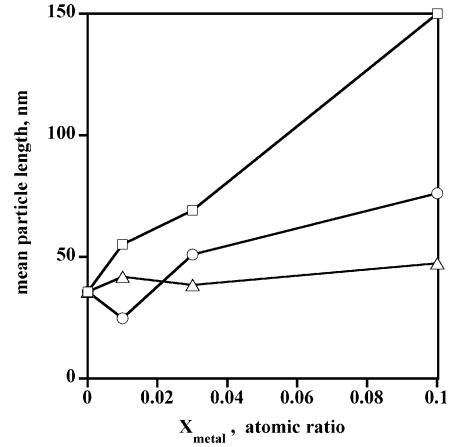

Figure 3. Mean particle length of the particles formed with Al(III) (○), La(△), and Fe(III) (□) by the coprecipitation method.

X_{metal} values in the surface layer and in the whole particles, respectively. X_s was estimated from the area intensity of XPS peaks of Ca(2p), Al(2p) La($3d_{5/2}$), and Fe($2p_{3/2}$), while X_w was assayed by the ICP-AES measurement after dissolving the particles in HNO_3 solution.[17] These values were reported in our previous work.[17] Therefore, the values of $X_s/X_w > 1$ indicate that the surface layer of the particles contains more metal than the bulk one. Hence, the large X_s/X_w values of the particles produced at $X_{Al} = 0.01$ (4.3) and $X_{La} = 0.01$ (2.2) suggest that Al(III) and La(III) are rich in the surface layer. As can be seen in Figure 1a, the Hap crystal possesses 10 Ca atoms and they are described as Ca(I) and Ca(II) according to their environments; four Ca(I) atoms (called columnar Ca atoms) occupy positions at levels *c*/2 and *c* and six Ca(II) atoms (called screw axis Ca atoms) occupy positions at levels *c*/4 and (3/4)*c* in sets

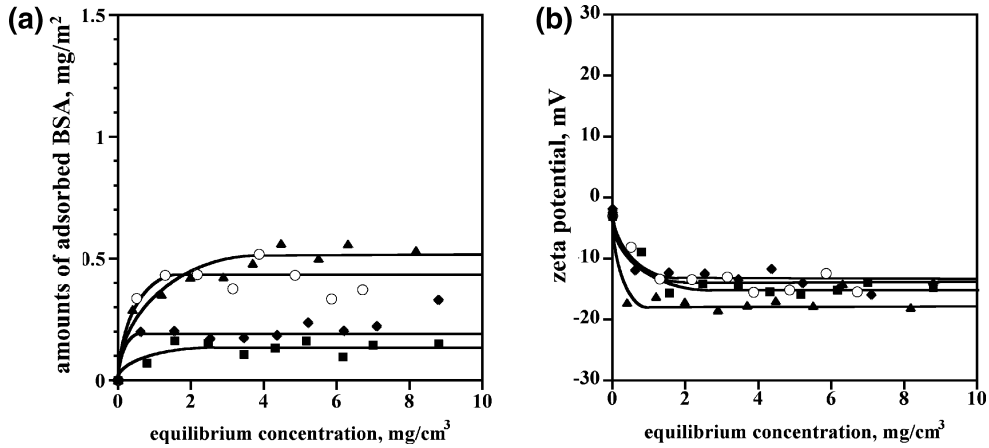

Figure 4. (a) Adsorption isotherms of BSA and (b) their zeta potential for Al(III)-substituted Hap particles. X_{Al}: (○) 0, (■) 0.01, (◆) 0.03, and (▲) 0.10.

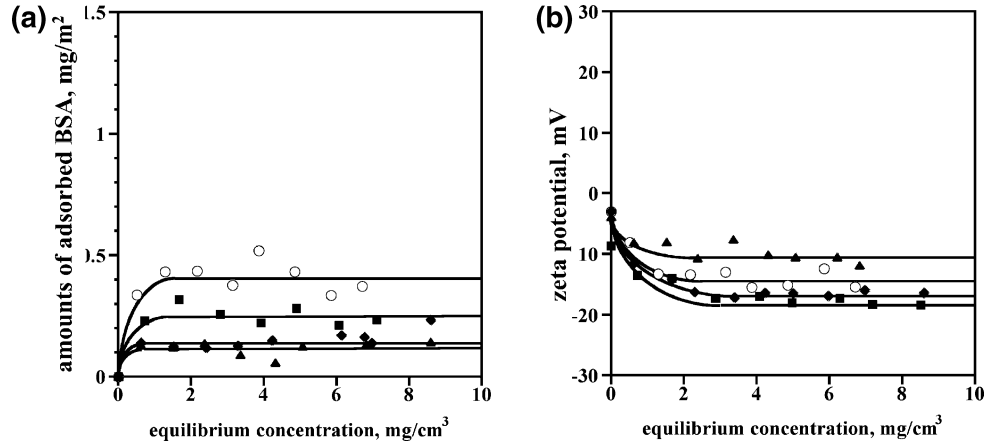

Figure 5. (a) Adsorption isotherms of BSA and (b) their zeta potential for La(III)-substituted Hap particles. X_{La}: (○) 0, (■) 0.01, (◆) 0.03, and (▲) 0.10.

of three. Therefore, it is hard to fix the position of substituted metal ions in the Hap crystal from the results only obtained in the present study. The S_W/S_N ratios, representing the surface hydrophilicity of the Hap particle, for Fe(III)-substituted particles are larger than Al(III)-substituted ones, but those for La(III)-substituted ones are less, indicating that the surface hydrophilicity of Fe(III)-substituted particles is high but that of La(III)-substituted ones is less.

The X-ray diffraction patterns of the products at different X_{metal} (data not shown) showed characteristic peaks of Hap (JCPDS 9-432), though the crystallinity of the materials was slightly lowered by increasing X_{metal} for all systems. However, since the adsorption behavior is only governed by the surface structure of the adsorbent but not by the whole crystal structure as described in the Introduction section, the change in the crystallinity of the Hap was neglected. Lattice expansion of Hap crystal by substituting the metal ions can also be expected. However, this effect was also ignored by the same reason.

Adsorption Behavior of BSA onto Al(III)-, La(III)-, and Fe(III)-Substituted Hap Particles. Adsorption isotherms of BSA onto the Al(III)-, La(III)-, and Fe(III)-substituted Hap particles are shown in Figures 4, 5, and 6 along with zp, respectively. All of the adsorption isotherms of BSA from 1×10^{-4} mol/dm^3 KCl solution are the Langmuirian type. The saturated amount of adsorbed BSA (n_s^{BSA}) for original-Hap (○) was 0.45 mg/m^2. The adsorption coverage of BSA (θ_{BSA}) on this system, defined as the ratio of the experimental amounts of adsorbed BSA (n_s^{BSA}) to the theoretical value, is 0.18. The latter value was estimated as 2.52 mg/m^2 by assuming a side-on adsorption of globular BSA molecules, which are prolate ellipsoids of 14×4 nm^2.[18] Since the solution pH of the system was ca. 8, BSA molecules are negatively charged. Therefore, the negative values of zp of this system were increased with an increase in the amount of adsorbed BSA. As is seen in Figures 4, 5, and 6, the n_s^{BSA} values are strongly dependent on X_{metal} in each system. In Figure 7, the n_s^{BSA} values are plotted as a function of X_{metal} in each metal system. The n_s^{BSA} values for the Fe(III) system are increased with an increase in X_{Fe}. The n_s^{BSA} value for the Fe(III)-substituted Hap particles obtained at $X_{Fe} = 0.10$ is 2.7-fold more than that that for the original-Hap particle, though that for the La(III) system is decreased to ca. 1/5. On the other hand, the n_s^{BSA} values for the Al(III) system are decreased with substitution of small amounts of Al(III), showing a minimum point at $X_{Al} = 0.01$, but they are increased again at X_{Al} over 0.03.

The authors previously reported that cations in solutions exert a binding effect between negatively charged Hap and BSA molecules by charge neutralization.[13,14] Hence, this point was first to be elucidated. To know the effect of cations dissolved from particles on the BSA adsorption behavior, we measured the contents of cations in solution by the ICP-AES measurement. In this experiment, we measured concentrations of cations in both the absence and presence of 1.0 mg/cm^3 BSA. The concentrations of Ca(II) and hetero metal ions dissolved from the particles are plotted as a function of X_{metal} in Figures 8 and 9, respectively. Here, the concentrations of cations are expressed

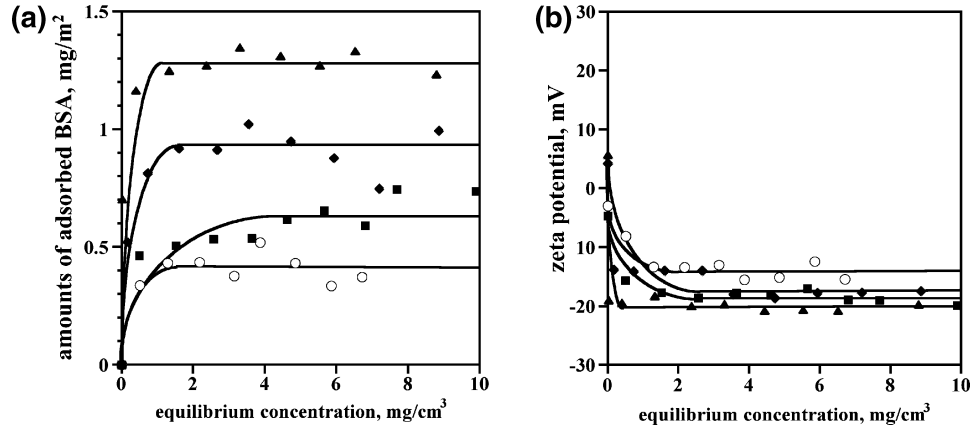

Figure 6. (a) Adsorption isotherms of BSA and (b) their zeta potential for Fe(III)-substituted Hap particles. X_{Fe}: (○) 0, (■) 0.01, (◆) 0.03, and (▲) 0.10.

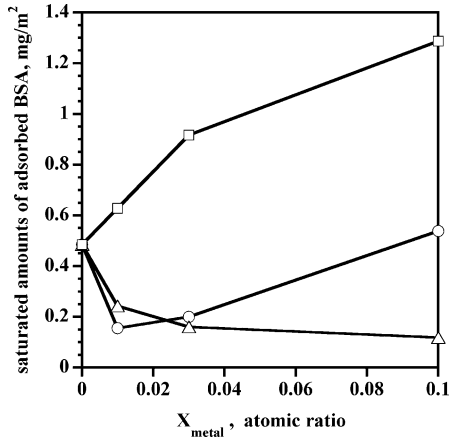

Figure 7. Changes of n_s^{BSA} as a function of X_{metal} for Al(III)-, La-, and Fe(III)-substituted Hap particles. Al(III) (○), La (△), and Fe(III) (□).

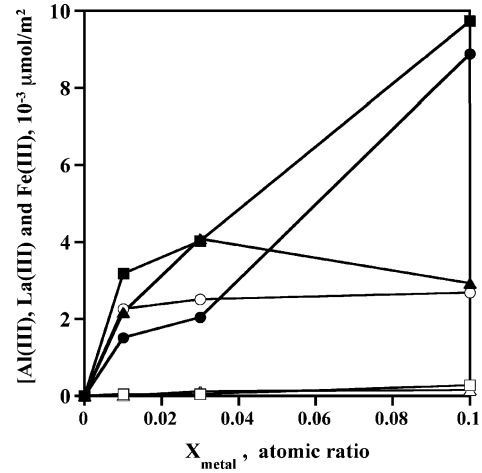

Figure 9. Changes of concentration of Al(III) (○,●), La(III) (△,▲), and Fe(III) (□,■) ions as a function of X_{metal} for each system. (○,△,□) in the absence of BSA (●,▲,■) in the presence of 1.0 mg/cm³ BSA.

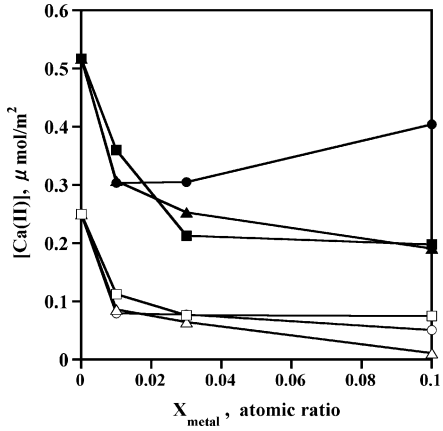

Figure 8. Changes of the concentration of Ca(II) ions as a function of X_{metal} for Al(III)- (○,●), La(III)- (△,▲), and Fe(III) (□,■)-substituted Hap particles. (○,△,□) in the absence of BSA; (●,▲,■) in the presence of 1.0 mg/cm³ BSA.

in μmol per unit m² using each S_N value. The open and closed symbols in Figures 8 and 9 are data obtained on the systems in the absence and presence of 1.0 mg/cm³ BSA, respectively. The calcium concentration, [Ca(II)], for the original-Hap particles in the absence and presence of BSA are 0.25 and 0.52 μmol/m², which coincides with the values reported in our previous study.[14] Since Ca(II) ions form complexes with the functional groups of BSA molecules in a solution, the [Ca(II)] values are increased in the presence of BSA. However, the [Ca(II)] values on all systems are decreased by an increase in X_{metal}. This result proves that the number of surface Ca(II) atoms was reduced by substitution with trivalent hetero metal ions. Since Ca is a constituent atom of Hap particle, Ca(II) ions dissolved from the particles do not exert a binder effect in any events.[14] As is seen in Figure 9, the concentrations of hetero metal ions obtained for the systems in the absence of BSA are low and Fe(III) and La(III) systems exhibit values of nearly zero, though they are increased in the presence of 1.0 g/cm³ BSA. Even though they increase, however, the concentration unit is 10^{-3} μmol/m², 100 times less than [Ca(II)], indicating mere trace amounts of hetero metal ions are dissolved from the particle surface. For example, 3.0×10^{-3} μmol/m² corresponds to 1.8×10^{-3} metal ions/nm². This result gives evidence that the cations dissolved from the particle surface do not induce the variation of n_s^{BSA} in Al(III)-, La(III)-, and Fe(III)-substituted Hap particles observed in Figure 7.

Next, we should consider the effects of surface structure and mean particle length on the n_s^{BSA} values. The authors have reported in a previous paper that the substitution ratio for the exchange of Ca(II) with trivalent ions was 1.0, 1.5, and 2.5 for Fe(III), Al(III), and La(III), respectively.[17] Taking account of the charge balance of Hap crystal, the theoretical substitution ratio for the exchange of Ca(II) with trivalent ions should be $3/2 = 1.5$. The ratio for Al(III) substitution is identical to the theoretical ratio, while the ratio for La(III) substitution is larger than the theoretical ratio and that for Fe(III) substitution is less,

signifying that the charge is not balanced in the substitution by La(III) and Fe(III). The substitution ratio of 1.5 obtained for the Al(III) system means that three Ca(II) atoms are substituted by two Al(III) atoms. Similarly, the substitution ratio of 1.0 obtained for the Fe(III) system suggests that all Ca(II) atoms are substituted by Fe(III) ones. Thus, in analogy with the Al(III) substitution system, it can be regarded that five Ca(II) atoms are exchanged by two La(III) atoms. These results indicate that the Fe(III)-substituted Hap particles possess excess positive charge, while the La(III) ones have excess negative charge. Therefore, to keep the charge balance, Fe(III) would be incorporated into the particles as lower valence ions such as hydroxo ions; $Fe(OH)^{2+}$ or $Fe(OH)_2^{+}$.[17] It has also revealed that, even with theoretical substituted ratio, Al(III) atoms are incorporated into the particles as hydroxo ions; $Al(OH)^{2+}$ or $Al(OH)_2^{+}$.[17] Therefore, surface Fe−OH and Al−OH bands besides P−OH ones were observed for these particles by in situ FTIR measurement.[17] On the other hand, the ICP-AES measurement revealed that La(III)-substituted Hap particles have no PO_4^{3-} deficiency. Therefore, we concluded in the previous paper that the substitution with La(III) accompanies the protonation of PO_4^{3-} to HPO_4^{2-} and $H_2PO_4^{-}$ and also OH^{-} to H_2O in the layer of the particles.[17] However, no surface La−OH group was detected for La(III)-substituted Hap particles for the charge balance.[17] The critical stability constant of La(III) ions complexed with OH^{-} ligands is 4.1, extremely lower than those of Al(III) (8.9) and Fe(III) (11.17),[19] indicating that La(III) ions are hard to hydrolyze. This fact accounts for the lack of surface La−OH groups, though the reason is still not clear at the moment. This absence of surface hydroxo La(III) ions corresponds to the low hydrophilicity of these particles (low S_W/S_N ratios of ca. 0.7 in Table 1) and strongly affected by the BSA adsorption behavior, as will be discussed in a next section.

Now we can discuss the change of n_s^{BSA} in Figure 7. We already revealed that n_s^{BSA} is strongly dependent on the mean particle length; the elongation of mean particle length increases the n_s^{BSA} value because the larger particles exhibit a greater fraction of **C** sites produced on predominantly crystal faces (*ac* and *bc*) along the *c*-axis.[11,12] Taking into account this fact, the increase of n_s^{BSA} by an increase in X_{Fe} can be ascribed to the growth of mean particle length along with the production of surface hydroxo ions to induce the hydrogen bond between the Fe(III)-substituted Hap surface and BSA molecules, though the number of original **C** sites established by Ca(II) atoms is reduced. Indeed, the S_W/S_N ratios of Fe(III)-substituted Hap particles exhibit over unity and are larger than other systems (Table 1), proving their high surface hydrophilicity.

In the case of La(III)-substituted Hap particles, the number of original **C** sites established by Ca(II) atoms are reduced by La(III) substitution but the mean particle length remains almost constant. Furthermore, surface La(III) hydroxo groups are absent in this system. Therefore, the reduction of n_s^{BSA} can be explained by both the unaltered mean particle length and their low surface hydrophilicity. The S_W/S_N ratios of this system certainly exhibit a low value of ca. 0.7 as discussed before. On the other hand, the change of n_s^{BSA} values by X_{Al} resembles that of the mean particle length; n_s^{BSA} and the mean particle length are decreased up to $X_{Al} = 0.01$, but they are increased after this minimum point (circle symbols in Figure 3). The results obtained imply that both the mean particle length and surface hydrophilicity are important factors for determining the adsorption amounts of BSA.

Conclusion

The effects of modification of Hap by Al(III), La(III), and Fe(III) ions on the BSA adsorption behavior were examined. The Hap particles were elongated on adding metal ions up to $X_{metal} = 0.10$, and the extent of the particle growth was in the order of La(III) < Al(III) ≪ Fe(III). The n_s^{BSA} values for the Fe(III) system exhibited a 2.7-fold increase in n_s^{BSA}, though those for the La(III) system are decreased to ca. 1/5. On the other hand, the n_s^{BSA} values for the Al(III) system are decreased with substitution of small amounts of Al(III) up to $X_{Al} = 0.01$, but they were increased again at X_{Al} over 0.03. The increase of n_s^{BSA} by an increase in X_{Fe} was explained by elongation of the mean particle length along with the production of surface hydroxo ions to induce the hydrogen bond between the Fe(III)-substituted Hap surface and BSA molecules. The reduction of n_s^{BSA} in the La(III) system was explained by both the unaltered mean particle length and their low surface hydrophilicity. The resemblance of the change of n_s^{BSA} values to that of the mean particle length in the Al(III) system suggested the importance of mean particle length. The obtained results strongly suggested that both the mean particle length and surface hydrophilicity are determining factors of the adsorption amounts of BSA.

References and Notes

(1) Kawasaki, T.; Takahashi, S.; Ikeda, K. *Eur. J. Biochem.* **1985**, *152*, 361–371.
(2) Kawasaki, T.; Niikura, M.; Takahashi, S.; Kobayashi, W. *Biochem. Int.* **1986**, *13*, 969–982.
(3) Kawasaki, T.; Ikeda, K.; Takahashi, S.; Kuboki, Y. *Eur. J. Biochem.* **1986**, *155*, 249–257.
(4) Chen, X.; Wang, Q.; Shen, J.; Pan, H.; Wu, T. *J. Phys. Chem. C* **2007**, *111*, 1284–1290.
(5) Shaw, W. J.; Campbell, A. A.; Paine, M. L.; Snead, M. L. *J. Biol. Chem.* **2004**, *279*, 40263–40266.
(6) Tiselius, A.; Hjertén, S.; Levin, Ö *Arch. Biochem. Phys.* **1956**, *65*, 132–155.
(7) Thomann, J. M.; Mura, M. J.; Behr, M. S.; Aptel, J. D.; Schmitt, A.; Bres, E. F.; Voegel, J. C. *Colloids Surf.* **1989**, *40*, 293–305.
(8) Kandori, K.; Sawai, S.; Yamamoto, Y.; Saito, H.; Ishikawa, T. *Colloids Surf.* **1992**, *68*, 283–289.
(9) Kandori, K.; Yamamoto, Y.; Saito, H.; Ishikawa, T. *Colloids Surf., A* **1993**, *80*, 287–291.
(10) Kandori, K.; Saito, M.; Saito, H.; Yasukawa, A.; Ishikawa, T. *Colloids Surf., A* **1995**, *94*, 225–230.
(11) Kandori, K.; Saito, M.; Takebe, T.; Yasukawa, A.; Ishikawa, T. *J. Colloid Interface Sci.* **1995**, *174*, 124–129.
(12) Kandori, K.; Shimizu, T.; Yasukawa, A.; Ishikawa, T. *Colloids Surf., B* **1995**, *5*, 81–87.
(13) Kandori, K.; Fudo, A.; Ishikawa, T. *Phys. Chem. Chem. Phys.* **2002**, *2*, 2015–2020.
(14) Kandori, K.; Masunari, A.; Ishikawa, T. *Calcif. Tissue Int.* **2005**, *76*, 194–206.
(15) Kandori, K.; Murata, K.; Ishikawa, T. *Langmuir* **2007**, *23*, 2064–2070.
(16) Kandori, K.; Mizumoto, S.; Toshima, S.; Fukusumi, M.; Morisada, Y. *J. Phys. Chem. B* **2009**, *113*, 11016–11022.
(17) Wakamura, M.; Kandori, K.; Ishikawa, T. *Colloids Surf., A* **2000**, *164*, 297–305.
(18) Squire, P. G.; Moser, P.; O'Konski, C. T. *Biochemistry* **1968**, *7*, 4261–4265.
(19) Smith, R. M.; Eartell, A. E. *Critical Stability Constants*; Plenum Press: New York, 1976; Vol. 4.

JP911783R